International Conference on Control, Engineering & Information Technology (CEIT'13)
Proceedings Engineering & Technology - Vol.1, pp. 58-63, 2013

Automatic Segmentation of Lumen in Intravascular Ultrasound Images Using Fuzzy Clustering and Active Contours

Hassen Lazrag [#1], Kamel Aloui [#2], Med Saber Naceur [#3]

[#] *LTSIRS, Ecole Nationale d'Ingénieurs de Tunis*
Campus d'El Manar à Tunis, Tunisie

[1] hassen.lazrag@laposte.net

[2] aloui_meteo@yahoo.fr

[3] naceurs@yahoo.fr

***Abstract*— Intravascular ultrasound (IVUS) imaging constitutes a widely used technique for coronary heart disease diagnosis and management of arterial atherosclerosis. The identification of lumen and media-adventitia boundaries in IVUS images is necessary for an efficient quantitative assessment of atherosclerotic plaques. In this paper, a new automated approach for lumen border detection is proposed. This method is based on fuzzy c-means algorithm and active contours model. First, the fuzzy c-means with spatial constraint algorithm is used to efficiently extract the regions of interest information of the IVUS image. Secondly, a novel level-set active contours algorithm is used to refine the segmentation and detect the lumen boundary. Experimented results achieved on textured IVUS images revealed that the proposed method gave good results.**

***Keywords*— Intravascular ulrasound, Lumen detection, Segmentation, Level-sets, Spatial fuzzy clustering**

I. Introduction

Intravascular ultrasound (IVUS) imaging has become rapidly one of the most famous technologies for coronary heart disease diagnosis and endovascular exploration. This technique consists in analyzing a several hundred of video images recorded with an ultrasound catheter. Therefore, it gives series of real-time, cross-sectional and high-resolution images of the explored blood vessels. Besides, IVUS modality offers visualization of atherosclerotic lesion morphology and precise measurements of vessel dimensions and cross-sectional areas. Manual analysis of the IVUS data is very long, fastidious and subject to intra- and inter-observer variabilities. These could be serious limitations against the clinical usage of IVUS technique. Furthermore, because of poor IVUS image quality due to the existence of speckle noise, imaging artifacts, calcifications shadowing and rupture of parts of the vessel wall, it is necessary to develop automatic segmentation methods.

Several approaches for automatic IVUS images segmentation have been developed so far, including texture analysis [1], active and surface contours [2,11], and knowledge-based graph searching [3]. In later approaches, specific lumen and media-adventitia segmentation was accomplished by utilizing active contours model principles in combination with other various techniques. Brusseau *et al.* [4] developed an automatic method for endominal contour detection based on an active contour evolving until it optimally separate regions in IVUS images with different statistical properties. Similarly, Filho *et al.* [5] employed a fuzzy clustering method for the extraction of the lumen boundary alone. Bovenkamp *et al*. [6] exploited a fully automatic multi-agent based system for luminal contour detection.

In this paper, we propose a robust approach to automatically detect lumen contour using three steps process (Fig. 1). The fuzzy spatial clustering is adopted in IVUS image to yield the initial contour of lumen border, then level set with edge stopping function refine the segmentation. This process allows the detection of the final lumen boundary.

The paper is organized as follows: Sections II-B and II-C depict about the theoretical background of the fuzzy c-means with spatial constraint algorithm, and the level sets scheme, respectively and Section II-D describes the lumen border detection. Experimental results and discussion are given in Section III, and the conclusion is summarized in Section IV.

II. Methods

A. IVUS Images Pre-processing

Three steps of preprocessing are used for the purpose of contour detection, which are: a) representation of the IVUS image in polar coordinates, b) detection of catheter region and replacing it by mean intensity value of the whole image (or totally removal of this zone), and c) edge-preserving smoothing. The preprocessing process is illustrated in Fig. 2.

Image representation in polar coordinates: The polar coordinates representation for image is essential to facilitate the efficient description of local image regions in the radial and tangential direction. This image representation is also applied for the contour initialization and an easier smoothing of the obtained contour. Therefore, the original IVUS image (in Cartesian coordinate [x, y]) is transformed into a polar coordinate image, where columns and rows correspond to angle θ and distance r from the center of gravity of the catheter, respectively. This polar image, denoted $I(r, \theta)$, is used for the remainder of the analysis process.

Detection of catheter region: Typical IVUS cross-sectional images show not only vessel wall and surrounding tissue, but also the border of the transducer of the catheter. The latter region defines a dead zone which contained no useful information. Having the diameter D of the catheter, the catheter-induced artifacts are easily removed by setting $I(r, \theta) = 0$ for $r < D/2+e$, where e denote a small constant. This region can be substituted with the average value of the whole image pixel intensities.

Edge preserving smoothing: The most famous edge-preserving smoothing algorithms used for IVUS images are median and anisotropic diffusion filtering. These filters tend to remove speckles and preserve the edge details. A median filter of window size 5 was finally used due to its robustness for speckle reduction and edge enhancement.

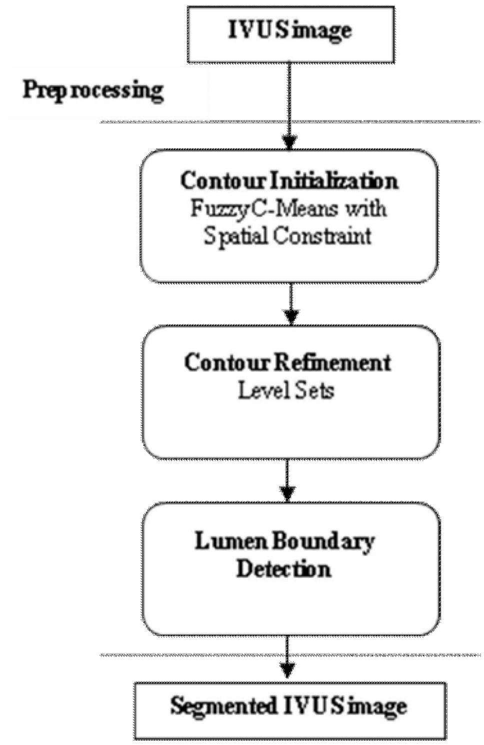

Fig. 1: The framework of the proposed luminal contour segmentation method

B. Fuzzy C-Means with Spatial Constraint

In this section we present the method used for the contour initialization procedure [12]. The method relies on fuzzy c-means (FCM) algorithm which is based on the minimization of an objective function $J(U, V)$ with respect to the membership functions u_{ik} and the centroids v_i, as follows

$$J(U,V) = \sum_{i=1}^{C} \sum_{k=1}^{N} (u_{ik})^m \|x_k - v_i\|^2 \qquad (1)$$

where x_k is the observation at pixel k, C is the number of clusters, and v_i is the i^{th} cluster center, $\|*\|$ is a metric norm (we use the Euclidean norm). The membership values $\{u_{ik}\}(k=1\ldots N)$ are constrained to be positive and to satisfy the condition: $\sum_{i=1}^{C} u_{ik} = 1$, $k=1,\ldots,N$, and $m > 1$ is a constant which controls the fuzziness of the resulting partition, it was set to 2 in this study.

The FCM technique is defined as an iterative optimization process that minimizes the distance between each image pixel and the prototypes. The cost function in (1) does not fully utilize any spatial information of the image. It has been shown in [8, 9] that the spatial constraint brings more robustness and efficiency to the classical fuzzy c-means technique. Therefore, a regularization term including the spatial constraint is incorporated into the FCM cost function. The new modified function can be expressed by the following equation:

$$J_M(U,V) = \sum_{i=1}^{C} \sum_{j=1}^{N} (u_{ij})^m \|x_j - v_i\|^2 + \alpha \sum_{i=1}^{C} \sum_{j=1}^{N} (u_{ij})^m e^{-\sum_{k\in\Omega}(u_{ik})^m} \qquad (2)$$

where Ω represents a set of neighbouring pixels, and α is a weight parameter to control the influence of the regularization term. The new cost function in equation (2) has two principal components. The first term is the same as the classical FCM algorithm; the second is a penalty component which is minimized when the membership value of neighbouring pixels in a specific cluster is high. Herein, the optimization problem in (2) with respect to U was solved by using the method of Lagrange multipliers. The authors [9] obtain the following membership update function

$$u_{ij} = \frac{1}{\sum_{p=1}^{C} \left(\dfrac{\|x_j - v_i\|^2 + \alpha e^{-\sum_{k\in\Omega}(u_{ik})^m}}{\|x_j - v_p\|^2 + \alpha e^{-\sum_{k\in\Omega}(u_{kp})^m}} \right)^{\frac{1}{m-1}}} \qquad (3)$$

The membership values (u_{pk}) of the neighbours centred on pixel (i,j) penalize the deviation of u_{ij} from the neighbourhood behaviour. For example, if a given pixel has a high membership value to a special cluster and its spatial neighbouring pixels have low membership values to this cluster, so that the penalty term may force this pixel to belong to the same cluster as its neighbouring pixels. The coefficient α controls the effect of the weighted regularization term. However, the prototype update equation of the cluster centres is the same as classical FCM.

$$v_i = \frac{\sum_{j=1}^{N} u_{ij}^m x_j}{\sum_{j=1}^{N} u_{ij}^m} \qquad (4)$$

The spatial FCM algorithm that incorporates the spatial information performs the same steps as the conventional fuzzy c-means clustering algorithm but the membership values were computed according to equation 3.

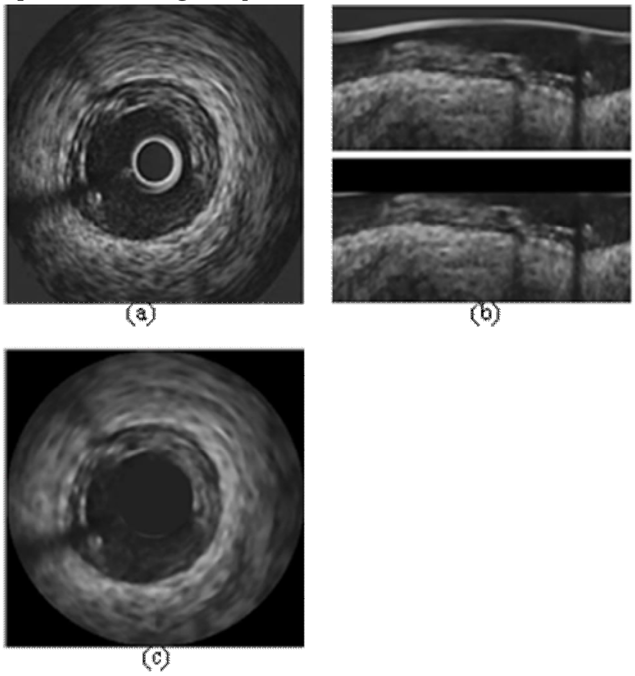

Fig. 2: The preprocessing process (a) original IVUS image, (b) polar image transform and catheter region removal, and (c) median filtered image.

C. Active Contour Model

In image processing, the active contours [13, 14] are self deforming dynamic interfaces that move under the effect of internal and external energy forces, towards the desired image features which we want to extract. For our proposed IVUS segmentation scheme, the geometric active contours developed further is based on a new level-set model; called level-set without re-initialization method (LSWR). This adopted approach is inspired from the work of Li et al. in [15]. The propagation of each interface or curve in the image is guided by internal and external forces. Indeed, the evolution of the proposed level set algorithm was directly derived from the gradient flow that minimizes the overall energy functional.

For a given image I, the desired borders, denoted by $\Gamma(t)$, are completely defined by the zero level-set function (LSF) $\varphi(x, y, t)$ satisfying

$$\begin{cases} \varphi(x,y,t) < 0 & (x,y) \text{ is inside } \Gamma(t) \\ \varphi(x,y,t) = 0 & (x,y) \text{ is at } \Gamma(t) \\ \varphi(x,y,t) > 0 & (x,y) \text{ is out side } \Gamma(t) \end{cases} \quad (5)$$

hence,

$$\mathbf{\Gamma}(t) = \{(x, y, t) \colon \varphi(x, y, t) = 0\} \quad (6)$$

To reach this goal, the authors in [15] proposed a functional energy that maintains the stability of the evolution of the LSF and moves the curves in the image toward the desired boundaries. This energy is defined as follows

$$E(\varphi) = \mu P(\varphi) + E_m(\varphi) \quad (7)$$

where $P(\varphi)$ is the internal energy (or the level-set regularization term) defined in the following, $\mu > 0$ is a coefficient to control the influence of penalizing the deviation of φ from an assigned distance function. The regularization term P maintains the stability of the level set function φ during its evolution, while the external energy E_m derives the LSF toward the image borders. The energy P is defined by the following expression

$$P(\varphi) = \int_\Omega (|\nabla\varphi| - 1)^2 dX \quad (8)$$

This metric is used to characterize how close a level-set function φ to a signed distance function in the two-dimensional domain Ω. It will play a crucial role in the proposed level set segmentation method. The external energy E_m is defined for a LSF φ as below

$$E_m(\varphi) = \lambda L(\varphi) + \nu A(\varphi) \quad (9)$$

where $\lambda > 0$ and υ are constants, and the facts $L(\varphi)$ and $A(\varphi)$ are defined by

$$L(\varphi) = \int_\Omega g\delta(\varphi(X))|\nabla\varphi(X)|dX, \quad (10)$$

and

$$A(\varphi) = \int_\Omega gH(\varphi(X))dX, \quad (11)$$

respectively, where δ is the Dirac function, and H is the Heaviside function. For numerical stability of the delta function, let define the classical regular approximations H_α and δ_α of the Dirac and Heaviside functions with $\alpha \in \Re+$

$$\delta_\alpha(s) = \frac{1}{2\alpha}\left(1 + \cos\frac{\pi s}{\alpha}\right) \quad (12)$$

and

$$H_\alpha(s) = \frac{1}{2}\left(1 + \frac{s}{\alpha} + \frac{1}{\pi}\sin\frac{\pi s}{\alpha}\right) \quad (13)$$

To guarantee the convergence of the LS curves and finish the segmentation process on the desired image contours, an edge indicator function g is used. This function is defined for an image I by

$$g(\nabla I) = \frac{1}{1 + |G_\sigma * \nabla I|^2} \quad (14)$$

where G_σ is the Gaussian kernel with a standard deviation σ, * is the convolution operator and ∇I is the gradient of the image I. To overcome the drawbacks of re-initialization process used in conventional level set, the authors in [15] proposed a standard method for the minimization of the above energy $E(\varphi)$ by using the gradient flow equation

$$\frac{\partial \varphi}{\partial t} = -\frac{\partial E}{\partial \varphi} \tag{15}$$

where $\partial E/\partial \varphi$ is the Gateaux derivative [16] of the total energy E. Accordingly, the gradient flow of the energy $E(\varphi)$ in (7) can be further expressed as

$$\frac{\partial \varphi}{\partial t} = \mu\left[\Delta\varphi - div\left(\frac{\nabla\varphi}{|\nabla\varphi|}\right)\right] + \lambda\delta(\varphi)div\left(g\frac{\nabla\varphi}{|\nabla\varphi|}\right) + vg\delta(\varphi),$$

$$\varphi_0(x,y) = \begin{cases} -C, & \varphi_0(x,y) < 0 \\ C, & \text{otherwise} \end{cases} \tag{16}$$

where C is a positive constant. During the propagation of the level-set curves according to the gradient flow, the second term in (10) attracts the LS interfaces towards the image borders while, the first term (regularisation term) penalizes φ to deviates from the signed distance function, eliminates the need for re-initialization process and has desirable advantages over the conventional level-set methods. First, the novel algorithm overcomes the limitations of the computationally expensive re-initialization procedure. Second, it permits the use of simpler and more efficient numerical scheme in its implementation.

D. Final Lumen Detection

A new active contours segmentation method is developed for lumen border detection in IVUS images. It begins with fuzzy clustering algorithm whose results are used to initiate level set segmentation. Then, the LSWR evolution is carried out to delineate the final lumen contour. This new approach automates the initialization procedure of the lumen border using a modified FCM with spatial constraints to determine the approximate contours of interest in IVUS image.

III. Experiments and discussion

The proposed IVUS segmentation algorithm was first evaluated with simulated images. It was also validated with manual method on real IVUS images.

A. Simulated IVUS images

Simulated images were conducted to evaluate the usefulness of the initial contour extraction using fuzzy clustering due to the fact that in these kinds of images the lumen contour is easily detected visually. Hence, they may be used to evaluate the accuracy of the new segmentation approach. The improvements are utilized to incorporate fuzzy clustering (SCFCM) into level set method for automatically initialize and detect the IVUS lumen boundary. Fig. 3 illustrates its performance on simulated IVUS image. These results demonstrated that detected lumen contours for the two simulated images were very close to the real lumen boundaries. They also showed the accuracy of our method in detecting lumen contours since the exact geometry of simulated images is known.

B. Real IVUS images

The in vivo coronary IVUS images used in this study was captured from different patients. Two images from these pull-packs were used to evaluate the accuracy of the proposed methodology for detecting IVUS lumen contour. Indicative results of our method were shown in Fig. 4, where the performance comparison between the automatically generated and the manual traced lumen contours is demonstrated. The results of the automated segmentation reveal sufficient agreement with the ground truth. Obviously, the proposed method seems trivial in detecting lumen boundaries for real IVUS images. However, the spatial fuzzy clustering cannot detect the external vessel boundary due to the much more smooth transition between the external vascular wall and the surrounding tissues and leakage of contrast.

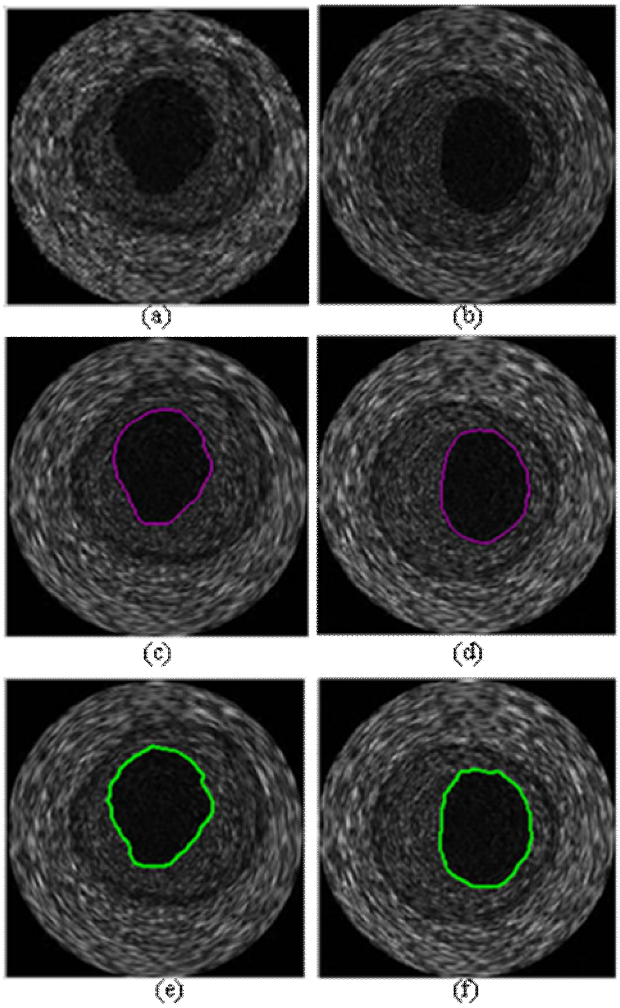

Fig. 3: Automatic lumen segmentation of two simulated IVUS images (a), (b) original images, (c), (d) initial lumen contours using modified fuzzy c-means (SCFCM) and (e), (f) the final lumen contours using level sets without re-initialization (LSWR).

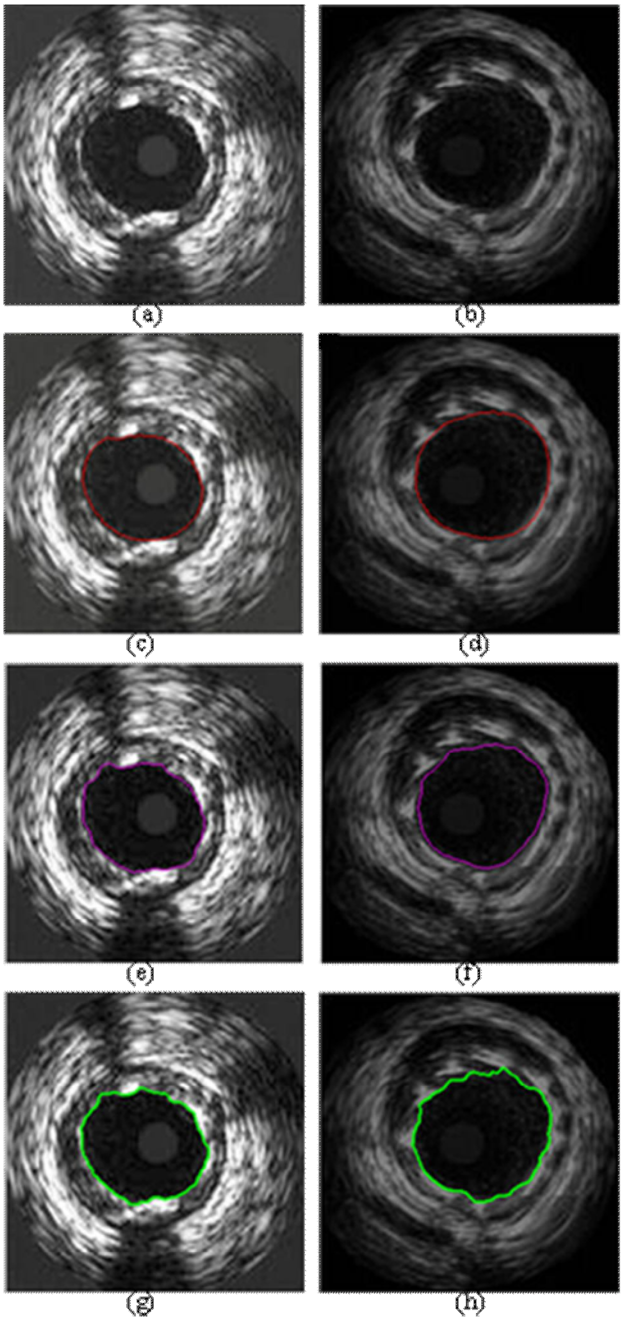

Fig. 4: Automatic lumen segmentation of two real IVUS images (a), (b) original images, (c), (d) manual traced lumen contours (e), (f) initial lumen contours using modified fuzzy c-means (SCFCM) and (g), (h) the final lumen contours using level sets without re-initialization (LSWR).

IV. Conclusion

A new segmentation method based on active contours and fuzzy clustering has been proposed for automatic lumen contour detection in IVUS images. The initialization process was performed automatically through a spatial information fuzzy c-means (SCFCM) algorithm. The modified FCM can approximate efficiently the boundary of interest. Therefore, the level-set curve evolution will start from a region close to the genuine lumen boundary and refine the final lumen contour. This has alleviated manual intervention. However, only the lumen contour was extracted with this system. In future research, it's interesting to extend this method for detection of media-adventitia contour, which is necessary for quantitative assessment of atherosclerosis. Hence, it would be very important that more high-level knowledge should be added to the system to control the motion of the level set contours.

References

[1] Mojsilovic, M. Popovic, N. Amodaj, R. Babic, M. Ostojic, Automatic segmentation of intravascular ultrasound images: a texture-based approach, *Ann. Biomed. Eng*. 25 (1997) 1059-1071.

[2] Sanz-Requena, R., Moratal, D., Garcıa-Sanchez, D.R., Bodı, V., Rieta, J.J., Sanchis, J.M.: Automatic segmentation and 3D reconstruction of intravascular ultrasound images for a fast preliminar evaluation of vessel pathologies. *Comput. Med. Imag. Graph*. 31 (2007) 71–80.

[3] Takagi, K. Hibi, X. Zhang, T. J. Teo, H. N. Bonneau, P. G. Yock et P. J. Fitzgerald. Automated contour detection for high-frequency intravascular ultrasound imaging: A technique with blood noise reduction for edge enhancement. *Ultrasound in Medecine and Biology*, 26(6):1033–1041, 2000.

[4] E. Brusseau, C.L. de Korte, F. Mastik, J. Schaar, A.F. van der Steen, Fully automatic luminal contour segmentation in intracoronary ultrasound imaging-A statistical approach, *IEEE Trans. Med. Imaging* 23 (2004) 554–566.

[5] S. Filho, E., Yoshizawa, M., Tanaka, A., Saijo, Y., Iwamoto, T. Detection of Luminal Contour Using Fuzzy Clustering and Mathematical Morphology in Intravascular Ultrasound Images. In: Proc. of 27th Annual International Conference of the IEEE Engineering in Medicine and Biology (EMBS), China, September 2005;3471–3474.

[6] E.G.P. Bovenkamp, J. Dijkstra, J.G. Bosch and J.H.C. Reiber, Multiagent segmentation of IVUS images, *Pattern Recognition*, vol.37, 2004, pp.647-663.

[7] Martin P, Refregier P, Goudail F, Guerault F. Influence of the noise model on level set active contour segmentation. *IEEE Transactions on Pattern Analysis and Machine Intelligence*. 2004;26:799–803.

[8] Hafiane A, Zavidovique B, Chaudhuri S. A modified fcm with optimal peano scans for image segmentation; IEEE ICIP; Genova, Italy: 2005.

[9] Chuang KS, Hzeng HL, Chen S, Wu J, Chen TJ. Fuzzy c-means clustering with spatial information for image segmentation. *Computerized Medical Imaging and Graphics*. 2006;30:9–15.

[10] Cai W, Chen S, Zhang D. Fast and robust fuzzy c-means clustering algorithms incorporating local information for image segmentation. *Pattern Recognition*. 2007;40:825–838.

[11] Giannoglou GD, Chatzizisis YS, Koutkias V, Kompatsiaris I, Papadogiorgaki M, Mezaris V, et al. A novel active contour model for fully automated segmentation of intravascular ultrasound images: in vivo validation in human coronary arteries. *Computers in Biology and Medicine*. 2007;37:1292–1302.

[12] B.N. Li, C.K. Chui, S.H. Ong, S. Chang, Integrating FCM and level sets for liver tumor segmentation, in: Proceedings of the 13th International Conference on Biomedical Engineering, (ICBME 2008), IFMBE Proceedings 23. (2009) 202–205.

[13] Sethian JA. Level Set Methods and Fast Marching Methods, Cambridge: Cambridge. New York: University Press; 1999.
[14] Osher S, Fedkiw R. Level Set Methods and Dynamic Implicit Surfaces. New York: Springer-Verlag; 2003.
[15] C. Li, C. Xu, C. Gui, M.D. Fox, Level set evolution without re-initialization: a new variational formulation, in: Proceedings of the 2005 IEEE Computer Society Conference on Computer Vision and Pattern Recognition (CVPR'05). (2005) 430–436.
[16] G. Aubert and P. Kornprobst, *Mathematical Problems in Image Processing: Partial Differential Equations and the Calculus of Variations*. New York: Springer-Verlag, 2002.